Diagnosis of Stator Windings Short-Circuits with PCA and Nuisance Attribute Projection

Pakedam Lare, Siyamak Sarabi, Claude Delpha, Demba Diallo

Diagnosis of stator windings short-circuits with PCA and Nuisance Attribute Projection

Pakedam LARE[1,2,3], Siyamak SARABI[1], Claude DELPHA[2], Demba DIALLO[3]

[1]*IFP Energies nouvelles, Institut Carnot IFPEN Transports Energie*, Rueil Malmaison, France
[2]*Université Paris-Saclay, CNRS, CentraleSupélec, L2S*, Gif-sur-Yvette, France
[3]*Université Paris-Saclay, CentraleSupélec, CNRS, GeePs*, Gif-sur-Yvette, France

Abstract—**Among the data-driven techniques for abnormalities detection in complex systems, Principal Component Analysis (PCA) is popular because of its simplicity and it does not require prior knowledge. However, the used of PCA is limited to stationary data. This work proposes a methodology to address this limitation. It consists of applying Nuisance Attribute Projection (NAP) in the preprocessing stage before the fault features are transformed with PCA to remove the nonstationarity effects due to the variable operating conditions. The proposal is evaluated to detect inter-turn short-circuits in the stator of a Permanent Magnet Assisted Synchronous Reluctance Motor (PMaSynRM) used in the powertrain of electric vehicles. The variances of the phase currents, computed in moving windows, are used as fault features. The results, obtained with seven fault severities and three load conditions, show that monitoring the Hotelling T^2 in the principal subspace leads to good performance, with probabilities of missed detection and false alarms lower than 0.02 and 0.05, respectively. To provide a safety metric, an estimate of the fault level is obtained with an analytical model of the evolution of the slope of the CUmulative SUM decision function with an accuracy greater than 97%.**

Index Terms—**Fault detection, PMaSynRM Inter-turn short-circuit fault, NAP**

I. INTRODUCTION

In process control of multivariate systems, Principal Component Analysis (PCA) is widely used because it requires no prior knowledge and is efficient to highlight the correlation among variables [1]. However, its application lies on the assumption that the variables are stationary (constant mean and variance over all the data time-series observations) and follow Gaussian distribution. [2]. Nevertheless, in a dynamic environment such electric vehicles, the variables have nonstationary properties mostly related to the varying operation conditions. To address this limitation, extensions based on the analysis of time-series segmentation with fixed or moving windows have been proposed. For example, the Dynamic Principal Component Analysis (DPCA) has been proposed in [3] to deal with autocorrelations. PCA is applied to a new expanded data matrix with time-shifted duplicate vectors for all variables. However, it has been shown in [4] that the resultant score variables of the DPCA can still be correlated. Consequently, the Probability of False Alarm (PFA) is higher when using the Hotelling's T^2 statistic as fault index. Multi-scale methods known as Multi-Scale PCA (MSPCA) have also been proposed

for feature extraction for dynamic systems: each variable is extended to different forms of the variable at different scales. For example, in [5] wavelets are used to decompose the variables into various scale representations. Then PCA is used to obtain the coefficients for wavelet reconstitution. The PCA algorithm is applied to the reconstructed data for fault detection. However, the accuracy of this methodology highly depends on the wavelet coefficients, which are not always optimal [6]. These extensions of the usual PCA come with some weaknesses like long response time, computational complexity, and their effectiveness is not always guaranteed. Determining the severity level of the defect is one of the crucial operations of the diagnosis. Indeed, it allows making the appropriate safety decision. The CUSUM decision function has proven to be an effective tool for estimating the severity of faults in electrical systems [7].

This work proposes a simple method for detecting short circuit faults between the turns of a PMaSynRM for different mechanical load conditions and levels of fault severity. The Nuisance Attribute Projection (NAP) is applied to the raw data in the preprocessing step to eliminate the data variabilities related to the load variation. This helps to get fault features that are only sensitive to the fault occurrence. The features are then normalized before being transformed with PCA to detect the fault. The effectiveness of the proposal will be evaluated in terms of probability of false alarm PFA and probability of missed detection (PMD). Once the defect is detected, the estimation of the severity level is obtained by the inversion of the analytical model of the evolution of the slope of the CUSUM decision function.

The rest of the paper is organized as follows: In Section II, after recalling the basics of PCA for fault diagnosis, NAP is presented, and the proposal is described. Section III presents the results and performance of the fault detection and fault severity estimation. Section IV concludes the paper.

II. FAULT DETECTION METHODOLOGY

Let us assume that the original data has N observations for n measured variables, that are arranged in a data matrix $\mathbf{X} \in \mathbb{R}^{N \times n}$. In this matrix, each vector is written as $\mathbf{x}_i^\mathsf{T} = [x_{1,i}, \ldots, x_{N,i}]$ where $x_{j,i}$ is the jth observation of the ith variable. In this approach, the collected data in healthy

operating conditions are used to build the reference model that will be used to evaluate the current data. The PCA and the NAP are first described, and the proposed fault detection strategy is further derived.

A. Principal Component Analysis for fault detection

Basically, PCA is used to reduce data dimensionality by grouping correlated variables in a set of new uncorrelated ones [8]. For a system with different physical variables of different magnitudes and scales, the original variable data set must be processed to give equal importance to all the variables. One way to achieve this is to give to all variables the same variance regardless of their magnitudes by using the normalization method. The normalization of vector $\mathbf{x}_i$ is done as follows:

$$
\begin{aligned}
\mu_{\mathbf{x}_i} &= \frac{1}{N} \sum_{j=1}^{N} x_{ji} \\
\sigma_{\mathbf{x}_i} &= \sqrt{\frac{1}{N-1} \sum_{j=1}^{N} \left(x_{ji} - \mu_{\mathbf{x}_i} \right)^2} \\
\bar{x}_{ij} &= \frac{x_{ji} - \mu_{\mathbf{x}_i}}{\sigma_{\mathbf{x}_i}}
\end{aligned}
\tag{1}
$$

where $\mu_{\mathbf{x}_i}$ and $\sigma_{\mathbf{x}_i}$ are the mean and standard deviation of $\mathbf{x}_i$ respectively, and $\bar{x}_{ij}$ is the re-scaled observation. In the rest of the paper, the scaled data are considered without bar notation for simplicity.

The normalized data is then subject to a linear transformation matrix $\mathbf{T}$ to express the variation in the observations such as $\mathbf{T} = \mathbf{X}\mathbf{P}$, with $\mathbf{T} \in \mathbb{R}^{N \times n}$ the principal component matrix and $\mathbf{P} \in \mathbb{R}^{n \times n}$ the eigenvectors matrix containing the eigenvalues λ_i of the correlation matrix $\boldsymbol{\Sigma}$ of $\mathbf{X}$ such as:

$$
\boldsymbol{\Sigma} = \mathbf{P} \wedge \mathbf{P}^{\mathsf{T}}
\tag{2}
$$

where $\wedge = diag(\lambda_1, \ldots, \lambda_n)$ is a diagonal matrix whose elements are sorted in decreasing magnitude order. The reduced l-dimensional space of the data is obtained by retaining only the principal components that correspond to the l-highest eigenvalues of the covariance matrix. They represent the feature space where most of the patterns in the data are represented (generally up to a given percentage of cumulated variance). The remaining components with the smallest eigenvalues represent the noise contribution. Once the number of components l to retain is determined, the eigenvectors matrix $\mathbf{P}$ and the principal component matrix $\mathbf{T}$ are partitioned into the form:

$$
\begin{aligned}
\mathbf{P} &= \begin{pmatrix} \hat{\mathbf{P}}_l & \widetilde{\mathbf{P}}_{n-l} \end{pmatrix} \\
\mathbf{T} &= \begin{pmatrix} \hat{\mathbf{T}}_l & \widetilde{\mathbf{T}}_{n-l} \end{pmatrix}
\end{aligned}
\tag{3}
$$

$\hat{\mathbf{X}}$ is the principal part of the data explained by the l first eigenvectors and the residual part $\widetilde{\mathbf{X}}$ is explained by the residual components [9]:

$$
\begin{aligned}
\hat{\mathbf{X}} &= \hat{\mathbf{P}}_l \hat{\mathbf{P}}_l^{\mathsf{T}} \mathbf{X} \\
\widetilde{\mathbf{X}} &= \widetilde{\mathbf{P}}_{n-l} \widetilde{\mathbf{P}}_{n-l}^{\mathsf{T}} \mathbf{X}
\end{aligned}
\tag{4}
$$

They respectively lead to the principal and residual subspaces used for fault diagnosis. A process monitoring with PCA uses Hotelling's T^2 and Q statistics also called Squared prediction error (SPE) to detect abnormal behaviors. Hotelling's T^2 and SPE represent the variability in the Principal Component Subspace (PCS) and the Residual Subspace (RS), respectively. T^2 can be expressed by using the estimated value $\breve{\boldsymbol{\Sigma}}$ of the correlation matrix as follows [10]:

$$
T^2 = \hat{\mathbf{X}}^{\mathsf{T}} \breve{\boldsymbol{\Sigma}}^{-1} \hat{\mathbf{X}}
\tag{5}
$$

Under normal conditions, if the data set is multivariate Gaussian distributed, the T^2 can be approximated by a $\chi2$ distribution with l degrees of freedom and a significance level $(1-\alpha)$. The system operation is considered healthy if $T^2 \leq T_\alpha^2$.

$$
T_\alpha^2 = \chi_{l,1-\alpha}^2
\tag{6}
$$

A variation of the variables' correlation indicates abnormal behavior. Under this condition, the sample matrix $\mathbf{X}$ increases its projection to the RS, and the magnitude of $\widetilde{\mathbf{X}}$ reaches abnormal values compared to those obtained during healthy conditions. SPE is the magnitude of $\widetilde{\mathbf{X}}$ and is written as:

$$
SPE = \| \widetilde{\mathbf{X}} \|^2
\tag{7}
$$

The process is considered healthy if the SPE statistic is under its control limit which is expressed as $SPE \leq SPE_\alpha$:

$$
SPE_\alpha = (\breve{\mu} + \breve{\sigma} z_{1-\alpha})^3
\tag{8}
$$

with $z_{1-\alpha}$ as the $(1-\alpha)$ significance level of a Gaussian distribution Φ. $\breve{\mu}$ and $\breve{\sigma}$ are the estimated mean and standard deviation of $SPE^{2/3}$ [10], respectively.

B. Nuisance Attribute Projection

Originally applied to reduce the signal interference from different channels in speaker recognition, it has been recently applied to condition-based maintenance to improve fault diagnostic. Its principle is explained graphically in Figure 1. The raw data are organized in the matrix $\mathbf{X}$ while $\mathbf{X}'$ is the data matrix from which the nuisances have been removed. Therefore, it is expected that $\mathbf{X}'$ is representative of the fault information. The transformation from $\mathbf{X}$ to $\mathbf{X}'$ is obtained with NAP as follows:

$$
\mathbf{X}' = \breve{\mathbf{P}} \mathbf{X}
\tag{9}
$$

where $\breve{\mathbf{P}} \in \mathbb{R}^{N \times N}$ is the projection matrix.

$$
\breve{\mathbf{P}} = \mathbf{I} - \sum_{i=1}^{d} \boldsymbol{\Delta}_{\mathbf{i}} \boldsymbol{\Delta}_{\mathbf{i}}^{\mathbf{T}}
\tag{10}
$$

where $\mathbf{I}$ is an $N \times N$ identity matrix, $\boldsymbol{\Delta}_{\mathbf{i}}$ represents the ith NAP direction, d is the number of NAP directions to be removed from the feature space and $d \leq N$. The parameter d can be determined by making a compromise between the computational complexity and the projection effect. Indeed, larger is d, better is the projection effect (nuisance mitigation) but higher is the computation time. The main objective of the NAP is to minimize the Projection Effect (**PE**) defined as follows:

$$
\mathbf{PE} = \sum_{i,j} W_{ij} \left\| \breve{\mathbf{P}} \cdot \mathbf{x_i} - \breve{\mathbf{P}} \cdot \mathbf{x_j} \right\|
\tag{11}
$$

W_{ij} is a weight coefficient that quantifies the relation between two feature vectors. It is defined as follows [11]:

$$W_{ij} = \begin{cases} 1 & \text{if } \mathbf{x_i} \neq \mathbf{x_j} \\ 0 & \text{otherwise} \end{cases} \qquad (12)$$

The minimization of $\mathbf{PE}$ in equation 11 can be transformed into finding the leading eigenvectors of the following eigen-problem [12]:

$$\mathbf{X}(\mathbf{W} - diag(\mathbf{WU}))\mathbf{X}^T \nu = \lambda \nu \qquad (13)$$

where $\mathbf{U}$ is an identity column vector, $\mathbf{W}$ the matrix of weight coefficients W_{ij}, λ the eigenvalues, and ν the eigenvectors. The solution to this problem is established in [11].
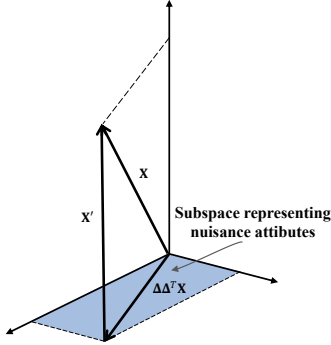

Fig. 1: Schematic diagram of NAP principle

C. Elimination of attributes related to varying operating conditions

In our proposed fault detection methodology, a preprocessing step based on NAP is added to the conventional PCA to address its limitation to deal with dynamic processes.
Initially, the stator three-phase currents are collected in the time domain under different mechanical loads. For feature extraction with less burden of large data, the sliding windows variance, on consecutive non-overlapping windows of fixed size is proposed to collect the data statistical features. The sliding windows variance is applied to the three-phase current signal in the time domain to get the data matrix $\mathbf{X}$. For a stator phase current signal $\mathbf{I^{(s)}}$, the jth observation of the ith variable $x_{j,i}$ of the matrix $\mathbf{X}$ is derived as follows [13]:

$$x_{i,j} = \frac{1}{\omega - 1} \sum_{I_m^{(s)} \in \Omega_j}^{N} \left(I_m^{(s)} - \dot{\mu} \right)^2 \qquad (14)$$

where $\dot{\mu}$ is the mean of the samples window $\Omega_j = \{I_{(j-1)\omega+1}^{(s)}, \ldots, I_{j\times\omega}^{(s)}\}$. To guarantee the data features properties, and to not violate the non-stationarity property of the data, the window size should be quite small. In this case study, the window size equals to the period of the phase current is used. For a variable speed drive the window size equivalent to the largest velocity series identified would be recommended.

The features are extracted for the healthy and test data using the moving variance. The NAP projection is at first computed

using the healthy data to get the model $\check{\mathbf{P}}$, which is independent of the dynamic load variations. To compute the projection matrix $\check{\mathbf{P}}$, the weight matrix $\mathbf{W}$ is generated to make the features independent. The minimization of the projection Effect ($\mathbf{PE}$) is then achieved by setting the columns of ν to be the σ most principal eigenvectors of the eigenvalue analysis in Equation 13. In our case, we set $\sigma = min(dim_{\mathbf{X}}, d)$, $dim_{\mathbf{X}}$ as the dimension of the features, and d as the number of the NAP directions. The model projection matrix $\check{\mathbf{P}}$ is used to remove from the healthy and actual features the effects of dynamic load variations. The transformed features are then used as inputs to the PCA for fault detection. The flowchart displayed in Figure 2 summarizes the proposal.

III. RESULTS AND DISCUSSIONS

In this section, the proposed methodology is applied to the detection of stator inter-turn short-circuits in a PMaSynRM.

A. Data generation and feature extraction

To evaluate the proposal, the model of the PMaSynRM presented in [14] and [15] is used. The characteristics of the electrical machine, and simulation parameters are displayed in Table I. The PMaSynRM winding under an inter-turn short-circuit fault in phase a is shown in Figure 3.

Under this faulty condition, the phase a current i_a is divided into: i_s the current in the defective part of the winding and i_f the current in the inter-turn fault's contact branch. L_{a1} and L_{a2} represent the inductances of the healthy and faulty sub-coils of the phase a winding, respectively. M_{a1b} and M_{a1c} are the mutual inductances between the healthy sub-coil L_{a1} and the coils L_b, and L_c, respectively. On the other hand M_{a1a2}, M_{a2b} and M_{a2b} represent the mutual inductances between the sub-coil L_{a2} and the healthy sub-coil L_{a1}, and coils L_b, and L_c, respectively.

TABLE I: The PMaSynRM characteristics

Motor characteristics	
Number of poles	8
Number of PMs per pole	5
Rated power [kW]	208
Maximum operating speed [rpm]	14000
Number of turns	8
Stator phase winding resistance value at $20°$ [$m\Omega$]	6.1
Simulation parameters	
Permanent Magnet flux amplitude [Wb]	6.24×10^{-2}
Moment of inertia [kgm^2]	0.0357
Input DC voltage amplitude [V]	412

Three load conditions ($\Gamma_1 = 18Nm$, $\Gamma_2 = 134Nm$, $\Gamma_3 = 260Nm$), each $3s$ long, are simulated at a controlled rotating speed of $1500rpm$. The short-circuits are emulated by changing the stator resistances and inductances. The faults of $1s$ duration are introduced after $1s$ for each case study. Seven severity levels are considered in this study, ranked from 2 to 8. This rank is related to the number of turns short-circuited in the winding of phase a.

Figure 4 displays the current flowing in the phase windings a of the PMaSynRM under healthy and faulty (fault severity level 2) conditions for the three different load cases.
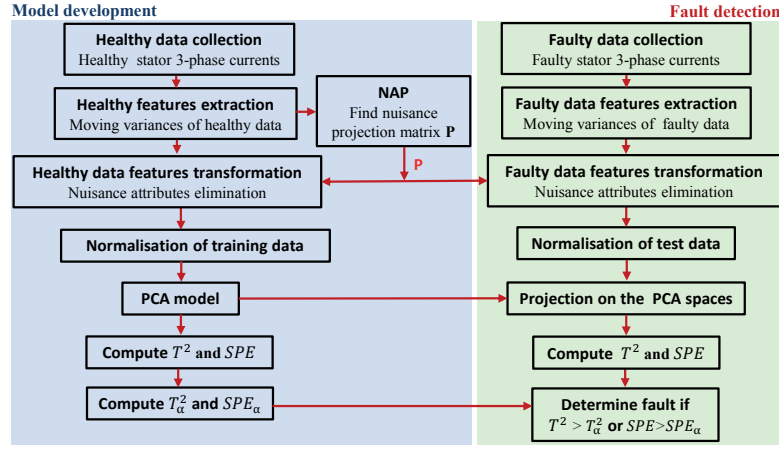
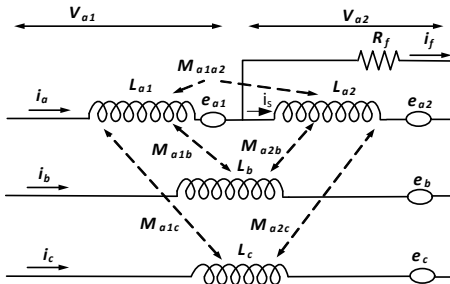Fig. 2: Flowchart of the NAP-based PCA methodology

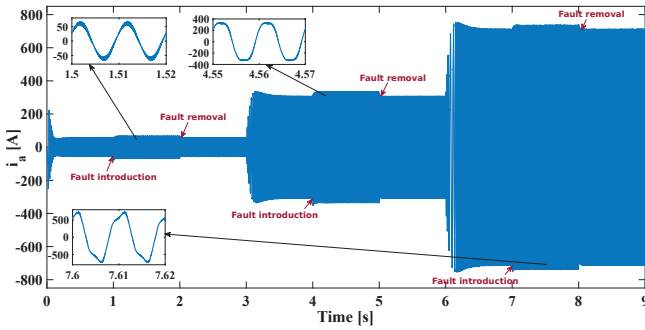Fig. 3: Stator windings circuit under an inter-turn fault

Fig. 4: Stator current in phase a under healthy and faulty (level 2) conditions
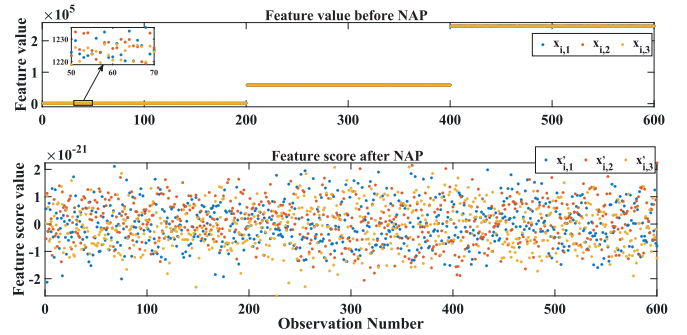

Fig. 5: Comparison of features before and after NAP

The new healthy features are used to design the model for the PCA. The threshold of the cumulative percentage variance is set to 90%. Figure 6 shows that the first two principal components capture 98.67% of the information. Therefore, in the PCA model, the principal subspace is spanned with the first two components while the third one defines the residual subspace.
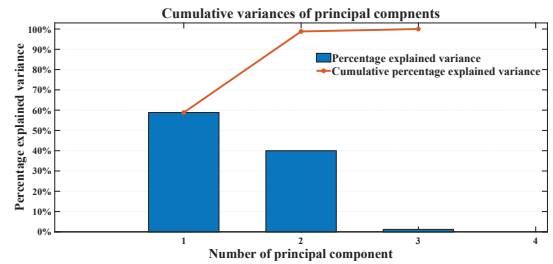
The fault characteristics are the variances of the phase currents. They are calculated using a moving window whose length is equal to the period of the currents, and stored in the data matrix $\mathbf{X}$.

B. Simulation results

As displayed in Figure 2, the procedure is composed of two parts: the first one (on the left side) uses the healthy data to obtain the projection matrix $\check{\mathbf{P}}$ that is used to transform the actual data (test data) for fault detection. The number of NAP directions is set to $d = 3$. Figure 5 displays for the healthy data the original features and the projected ones for three different loads. It can be clearly seen that after projection with the NAP, the new features are insensitive to load variations.

Fig. 6: Variance captured by each principal component

The Hotelling T^2 and the squared prediction error SPE will be used as fault indicators. The thresholds T_α^2 and SPE_α are set at $1-0.99$ confidence level, are computed for $\chi2$ and z distributions, respectively. The results for the fault level 2 are shown in Figure 7. The dashed lines represent the thresholds.

Figure 8 shows the overall performance comparison of the T^2 and SPE monitoring in terms of probability of missed
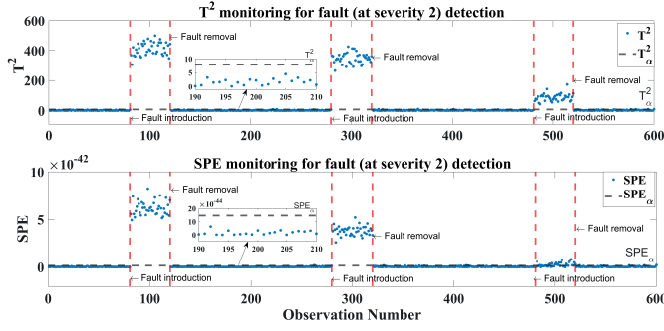
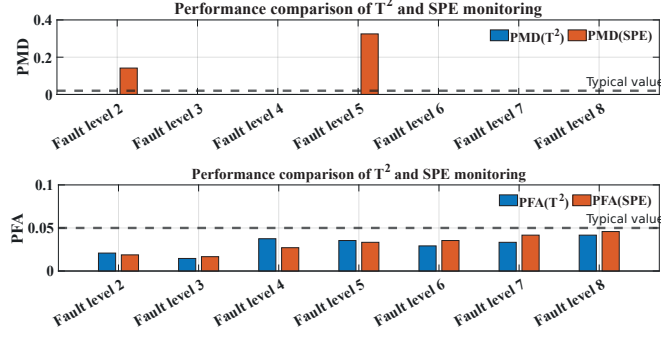Fig. 7: Fault level 2 detection with NAP-based PCA

Fig. 8: Performance of NAP-based PCA fault detection

fault detection PMD and probability of false alarm PFA for the seven fault severities and three loads. PMD and PFA are usually set to 0.02 and 0.05, respectively [16]. In Figure 8, these typical values are highlighted with dashed lines. For all case studies, it is observed that with the T^2, the fault detection performance is 100%. However, with SPE, the PMD is higher than the threshold for severities 2 and 5. These results show that for detecting inter-turn short circuits in an electrical machine, monitoring the Hotelling T^2 in the principal subspace is more efficient. This analysis indicates that, in our case study, the system modelling errors are projected onto the residual component which makes it less sensitive to the fault.

C. Fault estimation

Let us consider $\mu_{T_0^2}$ as the mean value of the selected fault index T^2 under healthy condition. As it can be observed in Figure 7 the average value undergoes an abrupt change to a new value denoted as $\mu_{T_1^2}$ when the defect appears. Under the assumption that the variance $\sigma_{T^2}^2$ of T^2 is constant, the instantaneous likelihood ratio $s(i)$ of the ith observation of the distribution of T^2 is given as follows [17]:

$$s(i) = \frac{\mu_{T_1^2} - \mu_{T_0^2}}{\sigma_{T^2}^2} \left(T^2(i) - \frac{\mu_{T_1^2} + \mu_{T_0^2}}{2} \right) \quad (15)$$

The CUSUM function S_N for the N observations of T^2 and the CUSUM decision law $\mathbf{D_{S_N}}$ are given as follows [17]:

$$\begin{aligned} S_N &= \sum_{i=1}^{N} s(i) \\ \mathbf{D_{S_N}} &= \left(S_{N_i} - \min_{1 \le t \le i} (S_{N_t}) \right) \end{aligned} \quad (16)$$

A fault is detected when $\mathbf{D_{S_N}}$ is greater than the threshold T_α^2. The top of the Figure 9 shows a clear change in the T^2, despite fluctuations, while the bottom of the figure shows the evolution of the CUSUM decision function for the fault level 2. The latter also provides a relevant fault indicator. Compared to T^2 monitoring shown in Figure 8, the CUSUM monitoring leads to similar performance.
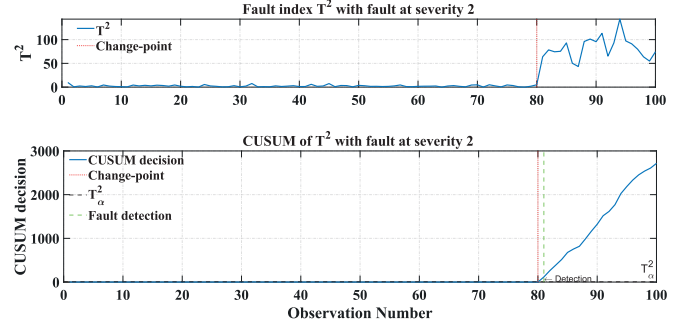

Fig. 9: CUSUM for fault monitoring

The severity of the faults varies from 0.25 to 1, corresponding to the number of short-circuited turns from 2 to 8. Figure 10 shows the evolution of the slope of the CUSUM decision function as a function of fault severity for the three load levels. It can be observed that the slope of the decision function increases monotonically with the severity of the defect regardless of the mechanical load. Therefore, it is a relevant characteristic that can be used to estimate the fault severity.
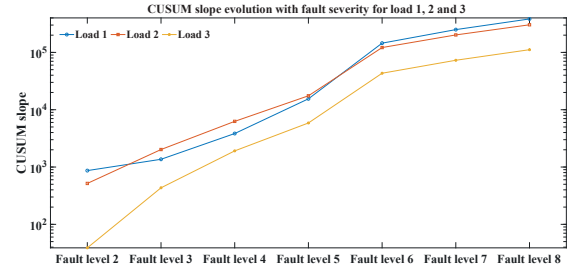

Fig. 10: Slope of CUSUM decision function

For the three load conditions, the evolution of the slope of the CUSUM decision dS_N as a function of fault severity f can be approximated by an exponential function as follows:

$$dS_N = ae^{b \times f} \quad (17)$$

where a and b are coefficients determined from the three load conditions. The upper section in Figure 11 shows the evolutions of the actual and analytical approximation of dS_N for the three load conditions. At the bottom, the actual and estimated fault severities are shown. The estimation performance
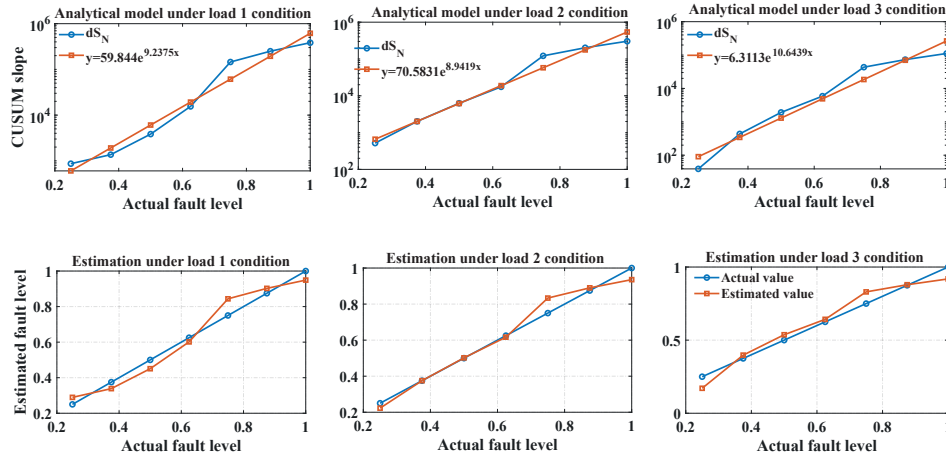
Fig. 11: Fault severity estimation

is evaluated through the Mean Square Error (MSE) and Correlation Coefficient (CC). The results are: $MSE = 0.00257$, $CC = 0.98$ for load 1, $MSE = 0.00173$, $CC = 0.98$ for load 2, and $MSE = 0.00306$, $CC = 0.97$ for load 3. This validates the approximation of the evolution of the slope of the CUSUM decision and the estimation of the fault severity with over 97% accuracy.

IV. CONCLUSION

In this paper, a fault detection methodology is proposed for inter-turn short-circuit fault monitoring in an electrical drive. An accurate model of the electrical powertrain is used to generate the dataset composed of measured phase currents under seven fault severities for three different loads. The variances of the currents flowing in the windings of the electrical machine are used as fault features. They are computed in a moving window whose length is equal to the period of the phase currents. The fault detection methodology combines the Nuisance Attribute Projection (NAP) with Principal Component Analysis (PCA). NAP is used in the preprocessing stage to remove from the fault features the effects of load variations, which are inherent in electric drives. This extra step only causes 2.12% increase of the computation time of the fault diagnosis. The probabilities of missed detection and false alarms (PFA and PMD) are computed to evaluate the method's performance when using the Hotelling T^2 or the Squared Prediction Error SPE as fault indexes. The results show that monitoring the T^2 in the principal subspace is the most efficient. An analytical model of the slope of the CUSUM decision function is derived, from which the fault severity is estimated. Compared to the actual fault level, the accuracy of the estimation is higher than 97%.

REFERENCES

[1] T. He, W.-R. Xie, Q.-H. Wu, and T.-L. Shi, "Process fault detection and diagnosis based on principal component analysis," in *International Conference on Machine Learning and Cybernetics*, Dalina, China, 2006, pp. 3551–3556.

[2] T. J. Rato and M. S. Reis, "Defining the structure of DPCA models and its impact on process monitoring and prediction activities," *Chemometrics and Intelligent Laboratory Systems*, vol. 125, pp. 74–86, 2013.

[3] W. Ku, R. H. Storer, and C. Georgakis, "Disturbance detection and isolation by dynamic principal component analysis," *Chemometrics and intelligent laboratory systems*, vol. 30, no. 1, pp. 179–196, 1995.

[4] U. Kruger, Y. Zhou, and G. W. Irwin, "Improved principal component monitoring of large-scale processes," *Journal of Process Control*, vol. 14, no. 8, pp. 879–888, 2004.

[5] B. R. Bakshi, "Multiscale PCA with application to multivariate statistical process monitoring," *AIChE journal*, vol. 44, no. 7, pp. 1596–1610, 1998.

[6] B. Malluhi, H. Nounou, and M. Nounou, "Enhanced multiscale principal component analysis for improved sensor fault detection and isolation," *Sensors*, vol. 22, no. 15, p. 5564, 2022.

[7] C. Delpha, D. Diallo, H. Al Samrout, and N. Moubayed, "Multiple incipient fault diagnosis in three-phase electrical systems using multivariate statistical signal processing," *Engineering Applications of Artificial Intelligence*, vol. 73, pp. 68–79, 2018.

[8] I. T. Jolliffe, *Principal component analysis for special types of data*. Springer, 2002.

[9] Y. Tharrault, G. Mourot, and J. Ragot, "Fault detection and isolation with robust principal component analysis," in *Mediterranean Conference on Control and Automation*, Ajaccio, France, 2008, pp. 59–64.

[10] S. Engelen, M. Hubert, and K. V. Branden, "A comparison of three procedures for robust PCA in high dimensions," *Austrian Journal of Statistics*, vol. 34, no. 2, pp. 117–126, 2005.

[11] W. M. Campbell, D. E. Sturim, D. A. Reynolds, and A. Solomonoff, "SVM based speaker verification using a GMM supervector kernel and NAP variability compensation," in *IEEE International conference on acoustics speech and signal processing proceedings*, vol. 1. IEEE, 2006, pp. I–I.

[12] H. Ma, S. Li, and Z. An, "A fault diagnosis approach for rolling bearing based on convolutional neural network and nuisance attribute projection under various speed conditions," *Applied Sciences*, vol. 9, no. 8, p. 1603, 2019.

[13] E. Villarreal-López, "A new scheme for multiple fault detection and isolation for rotational mechatronic systems, by means of analytical redundancy and adaptive filtering," *Dyna*, vol. 86, no. 209, pp. 40–48, 2019.

[14] P. Lare, S. Sarabi, C. Delpha, A. Nasr, and D. Diallo, "Stator winding inter-turn short-circuit and air gap eccentricity fault detection of a permanent magnet-assisted synchronous reluctance motor in electrified vehicle," in *International Conference on Electrical Machines and Systems (ICEMS)*. Gyeongju, Korea: IEEE, 2021, pp. 932–937.

[15] P. Lare, S. Sarabi, C. Delpha, and D. Diallo, "Modelling of a pma-synrm for the detection of inter-turn short-circuit," in *Conférence des Jeunes Chercheurs en Génie Electrique,(JCGE 2022)*, Le Croisic, France, 2022.

[16] P. Weber, D. Theilliol, C. Aubrun, and A. Evsukoff, "Increasing effectiveness of model-based fault diagnosis: A dynamic bayesian network design for decision making," *IFAC Proceedings Volumes*, vol. 39, no. 13, pp. 90–95, 2006.

[17] M. Basseville and I. V. Nikiforov, *Detection of abrupt changes: theory and application*. Prentice Hall Englewood Cliffs, 1993, vol. 104.